We are IntechOpen, the world's leading publisher of Open Access books Built by scientists, for scientists

2

Direct Torque control based multi-level inverter and artificial intelligence techniques of induction machine (DFIG)

LAMCHICH Moulay Tahar, LACHGUER Nora
University Cadi Ayyad/ Faculty of Sciences Semlalia/Department of Physic/Laboratory of Electronic and Instrumentation
Morocco

1. Introduction

With the enormous advances in converters technology and the development of complex and robust control algorithms, considerable research effort is devoted for developing optimal techniques of speed control for induction machines (IM). Also, induction motor control has traditionally been achieved using field oriented control (FOC). This method involves the transformation of the stator currents into a synchronously rotating dq reference frame that is aligned with one of the stator fluxes, typically the rotor flux. In this reference frame, the torque and flux producing components of the stator currents are decoupled, such that the d-axis component of the stator current controls the rotor flux magnitude and the q-axis component controls the output torque.

The implementation of this system however is complicated and furthermore FOC, in particularly indirect method, which is widely used, is well known to be highly sensitive to parameters variations, due to the feed-forward structure of its control system.

Another induction motor control technique known as a Direct Torque Control (DTC) was introduced in the mid 1980s, by Takahachi and Noguchi, for low and medium power applications; also Direct Self Control (DSC) was proposed by Depenbrock for high power applications.

DTC has a relatively simple control structure yet performs at least as good as the FOC technique. It is also known that DTC drive is less sensitive to parameters de-tuning (only stator resistor is used to estimate the stator flux) and provides a high dynamic performances than the classical vector control (fastest response of torque and flux).

This method allows a decoupled control of flux and torque without using speed or position sensors, coordinate transformation, Pulse Width Modulation (PWM) technique and current regulators. This type of command involves nonlinear controller type hysteresis, for both stator flux magnitude and electromagnetic torque, which introduces limitations such as a high and uncontrollable switching frequency. This controller produces a variable switching frequency and consequently large torque and flux ripples and high currents distortion.

The DTC is mostly used in the objective to improve the reduction of the undulations or the flux's distortion, and to have good dynamic performances. It's essentially based on a localization table which allows selecting the vector tension to apply to the inverter according to the position of the stator flux vector and of the direct control of the stator flux and the electromagnetic torque.

A wound rotor induction machine, used as a doubly fed induction generator (DFIG), is preferable for variable-speed wind turbine applications. The stator of DFIG is connected direct to the grid and the three-phase rotor windings link the grid by a bi-directional converter. The choice of control strategy incorporated can very depending wind turbine generators. In this chapter, the control scheme of the DFIG is DTC.

The general structure of the DFIG with DTC is represented by the following figure.

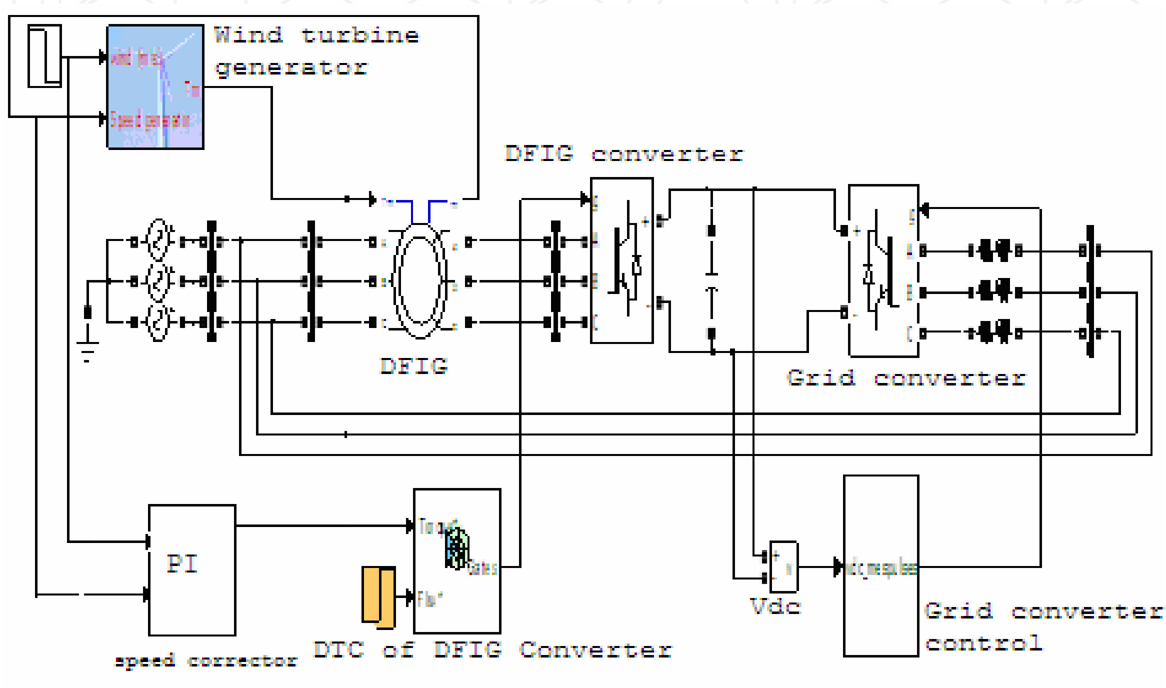

Fig. 1. General structure of the asynchronous motor with DTC and speed regulation

Also, the use of multi-level inverters and artificial techniques contribute to the performances amelioration of the induction machine control. In fact, the use of three level inverter (or multi-level inverter) associated with DTC control can contribute to more reducing harmonics and the ripple torque and to have a high level of output voltage.

Also, in last years, much interest has focused on the use of artificial intelligence techniques (neural networks, fuzzy logic, genetic algorithms,…) in identification and non linear control systems. This is mainly due to their ability learning and generalisation.

It become a number of papers appeared in literature interest to improving the performance of DTC applied to induction motor drive.

Among the different control strategies that were applied to achieve improved performance include:

- The switching frequency is maintained constant by associating the DTC to the space vector modulation;
- The space voltage is divided into twelve sectors instead of six with the classic DTC, and used some changes of the switching table.

Many researches have been performed using the multi-level inverter and, for example, some articles described a novel DTC algorithm suited for a three level inverter, and proposed a very simple voltage balancing algorithm for the DTC scheme.

Also, different other strategies using the artificial intelligence techniques were introduced, in order to achieve the objective that improving the performance of DTC:

- The direct torque control using a fuzzy logic controller to replace the torque and stator flux linkage hysteresis loop controller, space vector modulation, and fuzzy stator resistance estimator is more developed;
- The artificial neural network replacing the convectional switching table in the DTC of induction motor is also widely detailed.

In this chapter, all these points will be deeply developed and some simulation results, using Matlab/Simulink environment and showing the advantages of these approaches, will be presented. In the 1st section, we present the description of DTC method applied to the induction motor, as well as the simulation results will be illustrate the effectiveness of this method. In 2nd section, in the objective to improve the performance of DTC, the technique of multi-level inverter fed induction motor has been analyzed and simulation results show the performance of this approach. In 3rd section, we present the fuzzy logic direct torque control with two approaches: pulse width modulation and space vector modulation, also a model of artificial neural network is applied in DTC.
In the latest sections, the association of three-level inverter with fuzzy/Neural speed corrector for direct torque control of induction motor is developed.

2. Direct flux-torque control fundamentals

The direct torque control is principally a non-linear control in which the inverter switching states are imposed through a separate control of stator flux and electromagnetic torque of the motor. The inverter command is instantaneous and it replaces then the decoupling through the vectorial transformation. One of the most important characteristics of the DTC is the non-linear regulation of stator flux and electromagnetic torque with variables structures or by hysteresis.
The flux regulation is imperative for an efficient control of the induction machine torque and in the DTC, the stator flux regulation is chosen because it's easier to estimate, and partly it has a faster dynamics than the rotor flux. By adjusting the stator flux, we also adjust the rotor flux.
As in the other control methods, which use a direct regulation of the flux, the flux nominal value is imposed as a constant reference, for speeds lower than the nominal value. For higher speeds, a flux reference value, decreasing proportionally with speed; is imposed. On the other hand, the quality of rotation speed, and/or position, control of the modern actuators depends directly on the toque control.

2.1 Stator flux control

The IM equations, in a stator reference frame, are defined by:

$$\begin{cases} \overline{V}_s = R_s\,\overline{I}_s + \dfrac{d\overline{\phi}_s}{dt} \\ \overline{V}_r = 0 = R_r\,\overline{I}_r + \dfrac{d\overline{\phi}_r}{dt} - j\omega\,\overline{\phi}_r \\ \overline{\phi}_s = L_s\,\overline{I}_s + M_{sr}\,\overline{I}_r \\ \overline{\phi}_r = L_r\,\overline{I}_r + M_{sr}\,\overline{I}_s \end{cases} \qquad (1)$$

where R_s and R_r are the stator and rotor resistances.
L_s and L_r are the mutual stator and rotor inductances.
The stator flux is estimated from the measure of stator current and voltage and their transformation in the $\alpha\beta$ subspace. So:

$$\Phi_{s\alpha} = \int_0^t (V_{s\alpha} - R_s I_{s\alpha})dt \qquad \Phi_{s\beta} = \int_0^t (V_{s\beta} - R_s I_{s\beta}) \tag{2}$$

The stator flux module and the linkage phase are given by:

$$\Phi s = \sqrt{\Phi_{s\alpha}^2 + \Phi_{s\beta}^2} \qquad \alpha_s = arctg\left(\frac{\phi_{s\beta}}{\phi_{s\alpha}}\right) \tag{3}$$

On a sampling period T_e, and by neglecting the term $(R_s I_s)$ in equation of stator flux, valid hypothesis for high speeds, the evolution of this last one is given by the vector Vs during Te :

$$\Delta\Phi_s = \Phi_s - \Phi_{s0} = V_s T_e \tag{4}$$

Φ_{s0} is the initial stator flux at the instant t_0.
So, the variation of the stator flux is directly proportional to the stator voltage, thus the control is carried out by varying the stator flux vector by selecting a suitable voltage vector with the inverter.
A two level hysteresis comparator could be used for the control of the stator flux. So, we can easily control and maintain the flux vector Φ_s in hysteresis bound as shown in Figure.2.
The output of this corrector is represented by a Boolean variable $cflx$ which indicates directly if the amplitude of flux must be increased $(cflx = 1)$ or decreased $(cflx = 0)$ so as to maintain: $\left|(\Phi_s)_{réf} - \Phi_s\right| \le \Delta\Phi_s$, with $(\Phi_s)_{réf}$ the flux reference value and $\Delta\Phi_s$ the width of the hysteresis corrector.

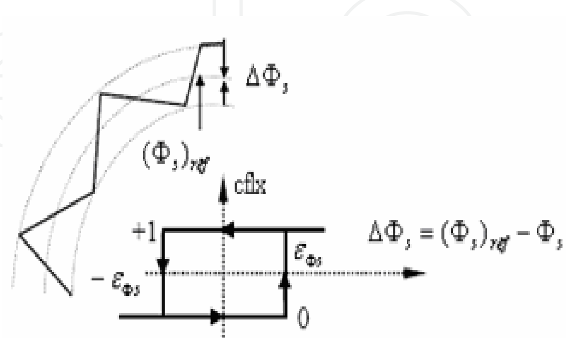

Fig. 2. Flux hysteresis corrector

2.2 Torque control

The electromagnetic torque expression is defined as follows, where γ represents the angle between the rotor and stator flux vectors:

$$\Gamma_{elm} = p\frac{L_m}{\sigma L_s L_r}\|\Phi_s\|\|\Phi_r\|\sin(\gamma) \tag{5}$$

where p is the number of pole pair
L_m : mutual inductance
σ : leakage coefficient (Blondel coefficient)
We deduct that the torque depends on the amplitude and the position of stator and rotor flux vectors.
On the other hand, the differential equation linking the stator flux and the rotor flux of motor is given by:

$$\frac{d\Phi_r}{dt} + (\frac{1}{\sigma\tau_r} - j\omega)\Phi_r = \frac{L_m}{\sigma\tau_r L_s}\Phi_s \tag{6}$$

From this equation, the flux Φ_r tracks the variations of the flux Φ_s with a time constant $\sigma\tau_r$.
In controlling perfectly the stator flux vector, from the vector V_s, in module and in position, we can control the amplitude and the relative position of the rotor flux vector and consequently the electromagnetic torque. This is possible only if the command period T_e of the voltage V_s is very lower to time constant $\sigma\tau_r$.
The expression of the electromagnetic torque is only obtained from the stator flux components $\Phi_{s\alpha}$, $\Phi_{s\beta}$ and currents $I_{s\alpha}$, $I_{s\beta}$:

$$\Gamma_{elm} = \Phi_{s\alpha} I_{s\beta} - \Phi_{s\beta} I_{s\alpha} \tag{7}$$

For the control of the electromagnetic torque, we can use a three level hysteresis comparator which permits to have the two senses of motor rotation. The output of this corrector is represented by a Boolean variable $Ccpl$ indicating directly if the amplitude of the torque must be increased, decreased or maintained constant $(ccpl = 1, -1, 0)$.

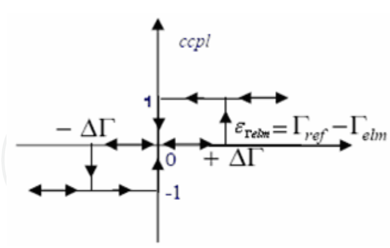

Fig. 3. Three level hysteresis comparator

2.3 Control strategy of DTC based two-level voltage inverter

Direct Torque Control of IM is directly established through the selection of the appropriate stator vector to be applied by the inverter. To do that, in first state, the estimated values of stator flux and torque are compared to the respective references, and the errors are used through hysteresis controller.
The phase plane is divided, when the IM is fed by two-level voltage inverter with eight sequences of the output voltage vector, into six sectors.

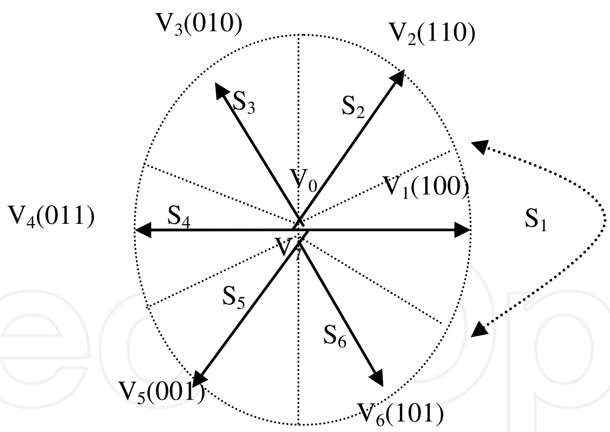

Fig. 4. Stator vectors of tensions delivered by a two level voltage inverter

When the flux is in a sector (i), the control of flux and torque can be ensured by the appropriate vector tension, which depends on the flux position in the reference frame, the variation desired for the module of flux and torque and the direction of flux rotation:

	Φs increase, Γ_{elm} increase	Φs increase, Γ_{elm} decrease	Φs decrease, Γ_{elm} increase	Φs decrease, Γ_{elm} decrease
Vector tension selected	V_{i+1}	V_{i-1}	V_{i+2}	V_{i-2}

Table 1. Selection of vector tension

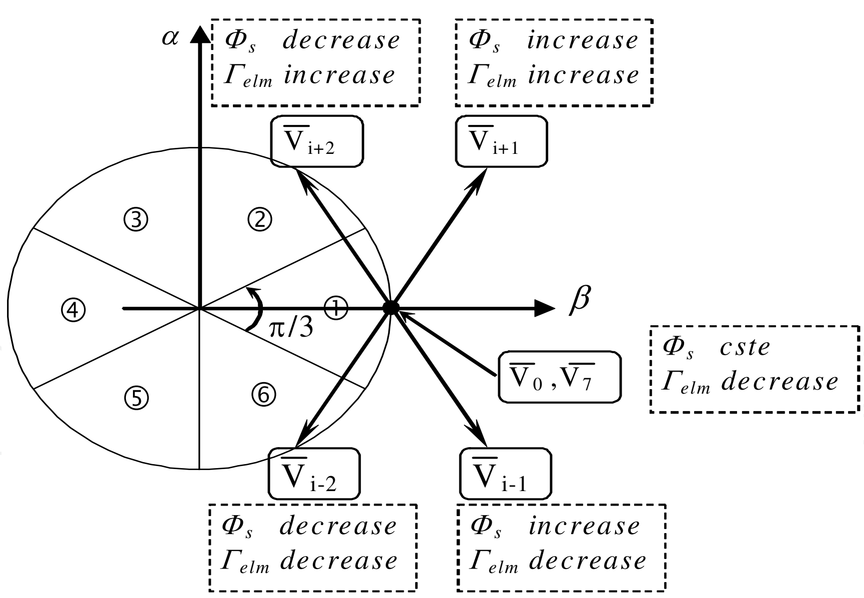

Fig. 5. Selection of vector tension

The null vectors (V_0, V_7) could be selected to maintain unchanged the stator flux.
According to the table 2, the appropriate control voltage vector (imposed by the choice of the switching state) is generated:

Cflx	ccpl	S_1	S_2	S_3	S_4	S_5	S_6
1	1	V_2	V_3	V_4	V_5	V_6	V_1
	0	V_7	V_0	V_7	V_0	V_7	V_0
	-1	V_6	V_1	V_2	V_3	V_4	V_5
0	1	V_3	V_4	V_5	V_6	V_1	V_2
	0	V_0	V_7	V_0	V_7	V_0	V_7
	-1	V_5	V_6	V_1	V_2	V_3	V_4

Table 2. Voltage vector selected (for each sector S_i)

The following figure shows the selected voltage vector for each sector to maintain the stator flux in the hysteresis bound.

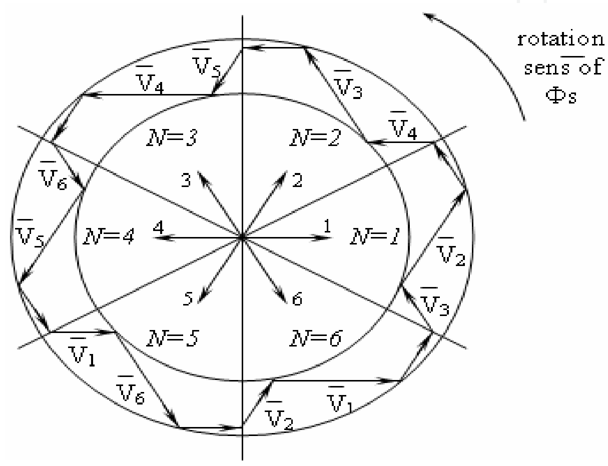

Fig. 6. Selection of vector tension

2.4 Simulation results

Simulations were performed to show the behavior of the Doubly Fed Induction generator connected to the grid by a bi-directional converter.

The torque reference value is deduced from the regulation of the wind generator speed according to the wind speed and using a PI corrector. In this example, we have used three levels of wind speed. We have chosen to present the results corresponding to the rotation speed evolution, the electromagnetic torque, the flux evolution in the αβ subspace and the stator currents.

The obtained simulation results show that:

- trajectory of the stator flux, represented by its two components in the αβ phase plane, is in a circular reference (Figure 7)
- phase current obtained by this strategy is quasi-sinusoidal (Figure 7)
- speed track its reference with good performance (Figure 8)
- overshoot on torque is limited by saturation on the reference value (Figure 8)

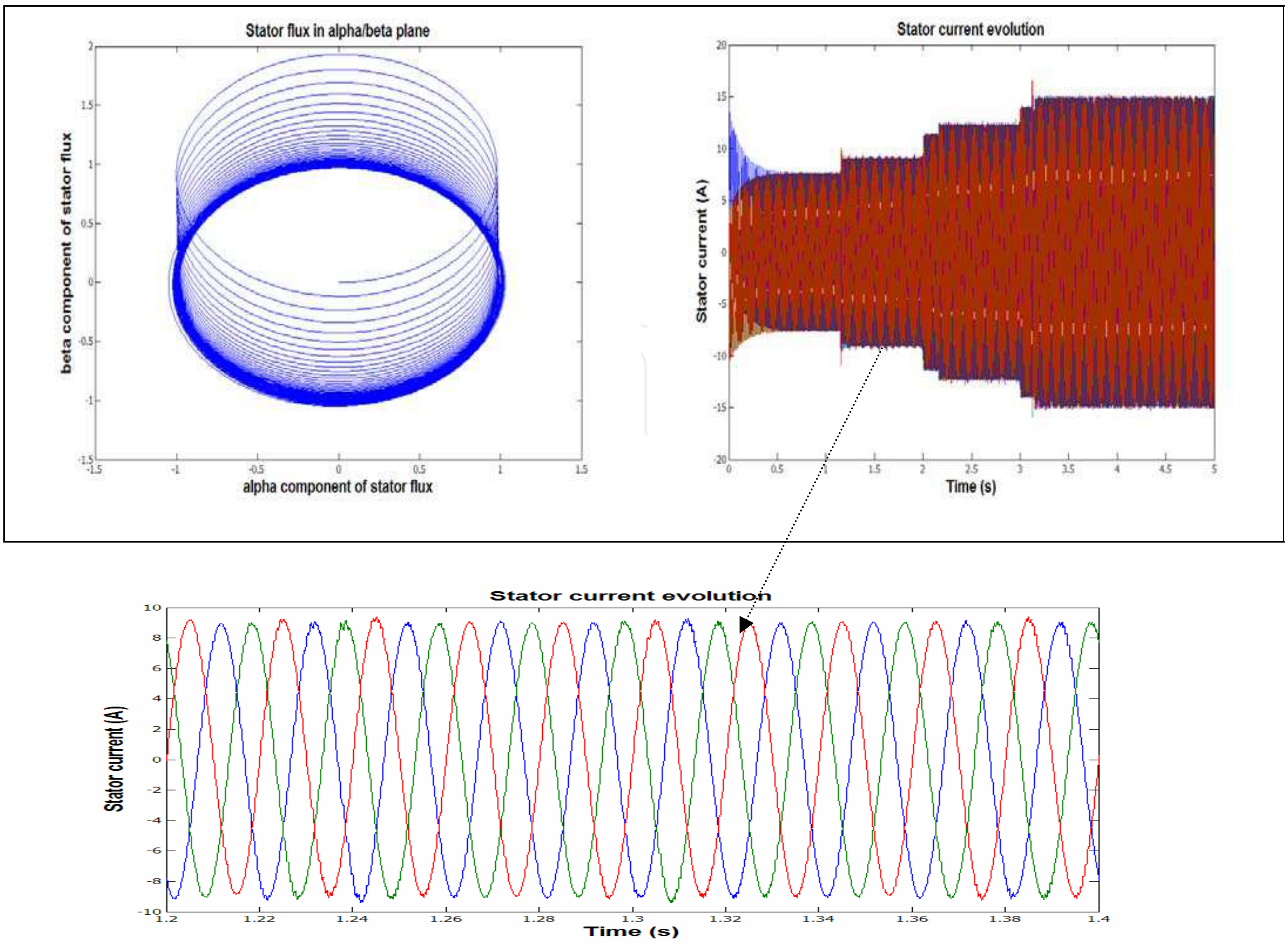

Fig. 7. Stator flux in the αβ phase plane and stator current time evolution

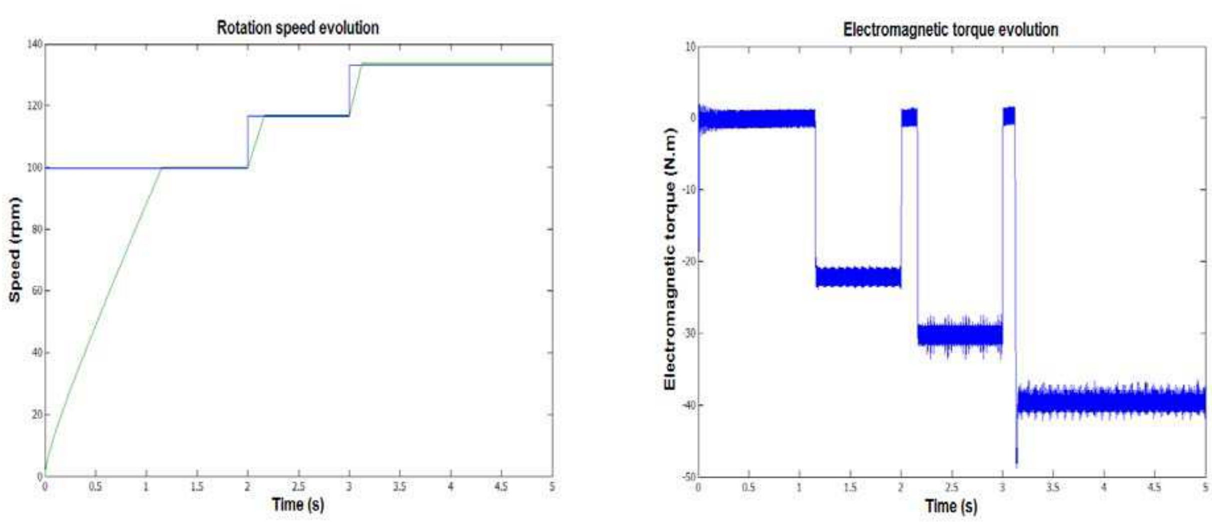

Fig. 8. Time evolution of speed and electromagnetic torque

3. DTC of Induction motor fed by multilevel inverter

Multilevel inverter present a big interest in the field of the high voltages and the high powers of the fact that they introduce less distortion and weak losses with relatively low switching frequency.

Three level inverter (or multilevel) can be used in the command DTC, what allows to reduce advantage the harmonics, to have a high level of output voltage and can contribute to more reducing harmonics and the ripple torque. In that case, the space of voltages is subdivided into twelve sectors (instead of six with the classic DTC) and by considering the method of the virtual vectors, three sections with small, medium and large vectors can be exploited.
We can also subdivide the space of voltages into only six sectors by adopting a technique which employs only twelve active voltage space vectors, corresponding to the small and large vectors and consequently without using the null or the medium space vectors.

3.1 Vectors tensions and phase level sequences of a three level inverter

The structure of the so called diode clamped three level inverter associated with the asynchronous motor is shown by figure 9.

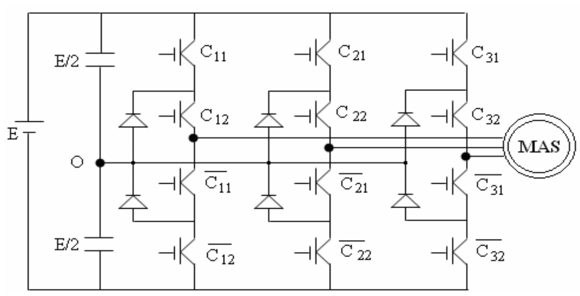

Fig. 9. Three level inverter structure

To analyze the potential generated by this three states inverter, every arm is schematized by three switches which permit to independently connect the stator inputs to the source potentials (represented by E/2, 0 and –E/2).
The interrupters (IGBTs) are switched in pairs consisting of (C_{11}, C_{12}), (C_{12}, $\overline{C}_{11}$) and ($\overline{C}_{11}$, $\overline{C}_{12}$). When, as example, the upper pair (C_{11}, C_{12}) is turned, the output is connected to the positive rail of the DC bus.
By making a transformation into $\alpha\beta$ (or dq) subspace, a resulting voltage vector is defined and associated to the spatial position of the stator flux. Then, the different states number of this vector is 19, since some of the 27 possible combinations produce the same voltage vector. There are three different inverter states that will produce the zero voltage vector and two states for each of the six inner voltage vectors (called small vector).
The figure 6 shows the various discreet positions, in the $\alpha\beta$ subspace, of the tension vector generated by a three level inverter.

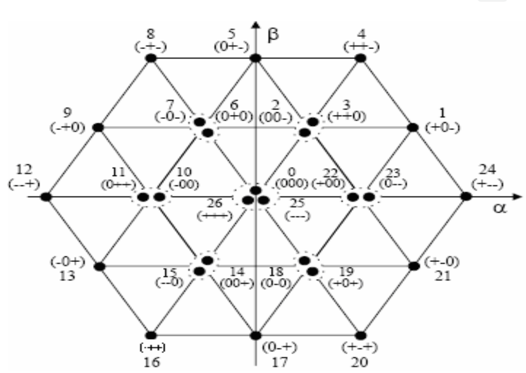

Fig. 10. Tension vectors generated by a three level inverter

3.2 Selection of voltages vectors for the control of the stator flux amplitude

As noted previously, the space evolution of the stator flux vector could be divided into twelve sectors i (Figure 11), instead of six with the classical DTC, with i= [1, 12] of 30° each, or into six sectors without using the medium vectors.
When the stator flux vector is in a sector i, the control of the flux and the torque can be assured by selecting one of 27 possible voltages vectors.
The difference between each of the inverter states that generate the same voltage vectors is in the way the load is connected to the DC bus. The analysis of the inverter states show that:

- the large vectors, such as V_{24} (+--), correspond to only the positive and negative rails of the DC bus are used and consequently have no effect on the neutral point potential;
- in the case of the medium vectors, the load is connected to the positive rail, neutral point and negative rail. The affect on the neutral point depends on the load current;
- there are two possible states of each of the small voltage vectors which can be used to control the neutral point voltage. As an example, small vector V_{22} (+00) causes capacitor C_1 to discharge and C_2 to charge and as a result the voltage of the neutral point starts to rise.

Depending on the stator flux position (sector) and the values of the outputs of torque and flux controllers, $\varepsilon_{\Phi s}$ and $\varepsilon_{\Gamma elm}$ respectively, the optimal vector is selected, from all available vectors.
The first sector could be chosen between -15° and 15° or 0° and 30°. Figure 11 present the space plane for the second case.

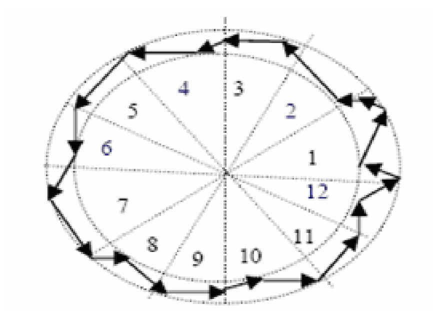

Fig. 11. Selection of vectors tensions Vs corresponding to the control of the magnitude Φ_s for a three level inverter.

3.3 Elaboration of the control switching table

The elaboration of the command structure is based on the hysteresis controller output relating to the variable flux (Cflx) and the variable torque (Ccpl) and the sector N corresponding to the stator flux vector position.
The exploitation of the first degree of freedom of the inverter, is made by the choice of vectors apply to the machine among 19 possibilities, during a sampling period. For the rebalancing of the capacitive middle point, the phase level sequence is chosen among all the possibilities associated with every voltage vector adopted. This establishes the second degree of freedom which must be necessarily used.

The switching table is elaborated depending on the technique adopted for the switching states choice.

3.3.1 Switching table based on a natural extension of classical DTC

This control scheme, which uses only twelve active voltage space vectors corresponding to the sections with small and large vectors and without using the null and medium space vectors, is a natural extension of classical DTC for a two level inverter.
We can consider the case where stator flux is achieved by using two-level hysteresis comparator and electromagnetic torque by using 4-level hysteresis. The inverter state is considered as high if the output of torque comparator is high or equal to two and otherwise, the state is low.
We can note that the choice of one of the two same states corresponding to the level low is relating to the capacitor voltage balancing.
Table 3 represents, in this case, the switching table.

Φ_s	Γ_{elm}	S_1	S_2	S_3	S_4	S_5	S_6
↑	↑↑	V_2^H	V_3^H	V_4^H	V_5^H	V_6^H	V_1^H
	↑	V_2^L	V_3^L	V_4^L	V_5^L	V_6^L	V_1^L
	↓	V_6^L	V_1^L	V_2^L	V_3^L	V_4^L	V_5^L
	↓↓	V_6^H	V_1^H	V_2^H	V_3^H	V_4^H	V_5^H
↓	↑↑	V_3^H	V_4^H	V_5^H	V_6^H	V_1^H	V_2^H
	↑	V_3^L	V_4^L	V_5^L	V_6^L	V_1^L	V_2^L
	↓	V_5^L	V_6^L	V_1^L	V_2^L	V_3^L	V_4^L
	↓↓	V_5^H	V_6^H	V_1^H	V_2^H	V_3^H	V_4^H

Table 3. Switching table with twelve active voltage space vectors

As shown by figure 10, the high vectors V_1^H, V_2^H, V_3^H, V_4^H, V_5^H and V_6^H are represented respectively by the configuration states of the inverter (+--),(++-),(-+-),(--+),(-++) and (+-+).

3.3.2 Switching table with twelve sectors

The space voltage vector diagram, for the three-level inverter, is divided into twelve sectors by using the diagonal between the adjacent medium and long vector.
According to the errors of torque and the stator flux linkage, the optimal vector is selected, from all 19 different available vectors (figure 12). The first sector is then chosen between -15° and 15°.

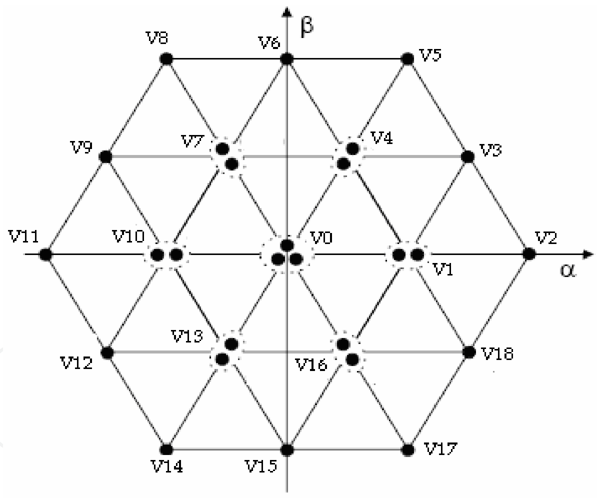

Fig. 12. Space voltage vector diagram (case of twelve sectors).

In analysing the effect of each available voltage vector, it can be seen that the vector affects the torque and flux linkage with the variation of the module and direction of the selected vector. For example, to increase the torque and flux V_3, V_4 and V_5 can be selected, but the action on the increasing torque and flux respectively of V_5 and of V_3 is the biggest.
Table 4 represents one of the solutions adapted to choice the optimal selected voltage vector for each sector. In this case, stator flux and torque are achieved by using respectively three levels and four levels hysteresis comparator. This technique doesn't use the null voltage vector for dynamics raisons.

Φ_s	Γ_{elm}	S_1	S_2	S_3	S_4	S_5	S_6	S_7	S_8	S_9	S_{10}	S_{11}	S_{12}
1	2	V_5	V_6	V_8	V_9	V_{11}	V_{12}	V_{14}	V_{15}	V_{17}	V_{18}	V_2	V_3
	1	V_3	V_5	V_6	V_8	V_9	V_{11}	V_{12}	V_{14}	V_{15}	V_{17}	V_{18}	V_2
	-1	V_{18}	V_2	V_3	V_5	V_6	V_8	V_9	V_{11}	V_{12}	V_{14}	V_{15}	V_{17}
	-2	V_{17}	V_{18}	V_2	V_3	V_5	V_6	V_8	V_9	V_{11}	V_{12}	V_{14}	V_{15}
0	2	V_7	V_7	V_{10}	V_{10}	V_{13}	V_{13}	V_{16}	V_{16}	V_1	V_1	V_4	V_4
	1	V_4	V_4	V_7	V_7	V_{10}	V_{10}	V_{13}	V_{13}	V_{16}	V_{16}	V_1	V_1
	-1	V_{16}	V_1	V_1	V_4	V_4	V_7	V_7	V_{10}	V_{10}	V_{13}	V_{13}	V_{16}
	-2	V_{13}	V_{16}	V_{16}	V_1	V_1	V_4	V_4	V_7	V_7	V_{10}	V_{10}	V_{13}
-1	2	V_8	V_9	V_{11}	V_{12}	V_{14}	V_{15}	V_{17}	V_{18}	V_2	V_3	V_5	V_6
	1	V_9	V_{11}	V_{12}	V_{14}	V_{15}	V_{17}	V_{18}	V_2	V_3	V_5	V_6	V_8
	-1	V_{12}	V_{14}	V_{15}	V_{17}	V_{18}	V_2	V_3	V_5	V_6	V_8	V_9	V_{11}
	-2	V_{14}	V_{15}	V_{17}	V_{18}	V_2	V_3	V_5	V_6	V_8	V_9	V_{11}	V_{12}

Table 4. Switching table with twelve sectors

This approach and others, for establishing of the optimal switching table and taking into account all the factors such as the capacitors balance, system dynamic and system reliability, must be deeply analysed and tested. Also, it's difficult, in this case, to select the optimal voltage vectors; however, the use of artificial intelligence techniques will add their superiority to some extent.

4. Direct torque control based fuzzy / neural network

By analyzing the structure of the switching table, we can notice that it can be translated in the form of fuzzy rules. Consequently, we can replace the switching table and the hysteresis comparator by a fuzzy system. The fuzzy character of this system allows flexibility in the choice of the fuzzy sets of the input and the capacity to introduce knowledge of the human expert there.
Also, as the DTC uses algorithms to select a large number of statements inverter switches, neural networks can accomplish this task after a learning phase. The neural network selector inputs will be proposed as the position of the flux stator vector, the error between its estimated value and the reference one, and the difference between the estimated and reference values of electromagnetic torque. The next figure shows an example of this structure.

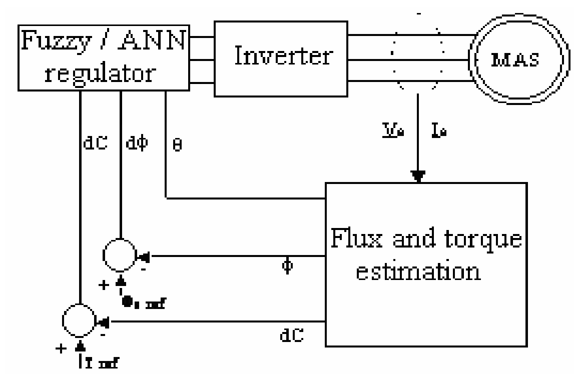

Fig. 13. Switching table based Fuzzy / ANN technique

4.1 Direct torque control based fuzzy logic

The principle of fuzzy direct torque control (FDTC) consists to replace, in conventional DTC, the torque and stator flux hysteresis controllers and the switching table by a fuzzy system.
In this case, two approaches can be presented to illustrate the strategy of FDTC of the induction motor fed by two-level inverter.
We can consider three variables input fuzzy logic controllers; the stator flux error, electromagnetic torque error and angle of stator flux, however, the choice of the output deferred according to the approach utilized. The output could be the voltage space vector, for FDTC based PWM, or the magnitude and argument of voltage vector for space vector modulation.

4.1.1 FDTC based Pulse Width Modulation (PWM)

The fuzzy logic controller blocks using PWM inverter is shown in the following figure. These blocks are composed of two main parts: fuzzification and fuzzy rules base, since no defuzzification is needed because, in this case, the output of fuzzy controller is the actual PWM voltage vector sequence and these states are directly the results of fuzzy rules.

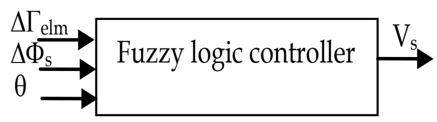

Fig. 14. Fuzzy logic controller based PWM

4.1.1.1 Fuzification

Based on the switching table of the conventional DTC, the universe of discourse for each three inputs of the fuzzy logic controller has been divided into: two fuzzy sets (NP), for stator flux error, three fuzzy sets (NZP), for electromagnetic torque error, and seven fuzzy sets ($\theta_0, \theta_1, \ldots, \theta_7$) for angle of flux stator.

These fuzzy sets are defined by the delta and trapezoidal membership functions and are presented by the following figure.

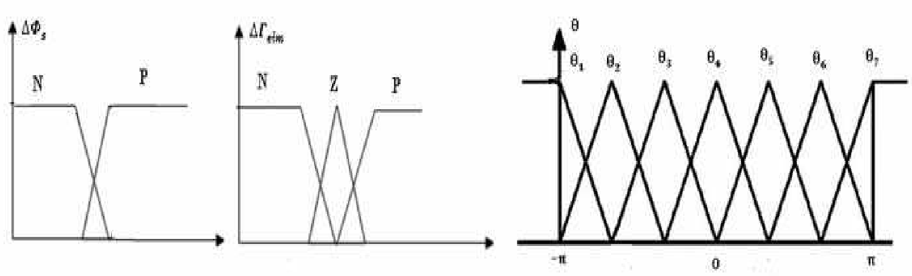

Fig. 15. Membership functions

4.1.1.2 Fuzzy rules base

The table can be expressed by fuzzy rules given by:

The i[th] rule R_i : if $\Delta\Phi$ is A_i and $\Delta\Gamma$ is B_i and θ is C_i then n is N_i.

A_i, B_i and C_i are the fuzzy sets of the variables $\Delta\Phi_s$, $\Delta\Gamma_{elm}$ and θ

n is the inverter switching state.

The inference method used is Mamdani's procedure based on min-max decision.

These rules are resumed by the following table.

	θ_1		θ_2		θ_3		θ_4		θ_5		θ_6		θ_7	
$\Delta\Phi_s$ / $\Delta\Gamma_{elm}$	P	N	P	N	P	N	P	N	P	N	P	N	P	N
P	V_5	V_6	V_6	V_1	V_1	V_2	V_2	V_3	V_3	V_4	V_4	V_5	V_5	V_6
Z	V_0	V_7	V_7	V_0	V_0	V_7	V_7	V_0	V_0	V_7	V_7	V_0	V_0	V_7
N	V_3	V_2	V_4	V_3	V_5	V_4	V_6	V_5	V_1	V_6	V_2	V_1	V_3	V_2

Table 5. Fuzzy rules

4.1.2 FDTC based Space Vector Modulation (SVM)

Using space vector modulation permit, in addition to the advantages obtained by the fuzzy logic controller (reduction of the torque, stator flux and current ripples and to get a fast torque response), to maintain constant the switching frequency. With this strategy two fuzzy controller of Mamdani could be used to control the magnitude and argument of voltage vector reference. For this technique, two controllers (next figure) are used concerning the variables magnitude and argument of vector tension.

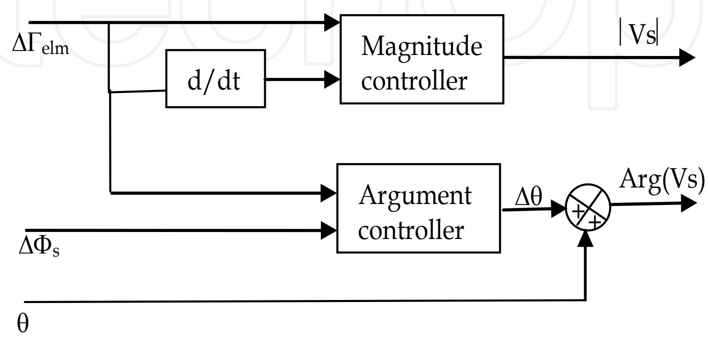

Fig. 16. Fuzzy logic controller based SVM

In the following figure, the membership functions of the variables ΔΦs and $\Delta\Gamma_{elm}$ are presented.

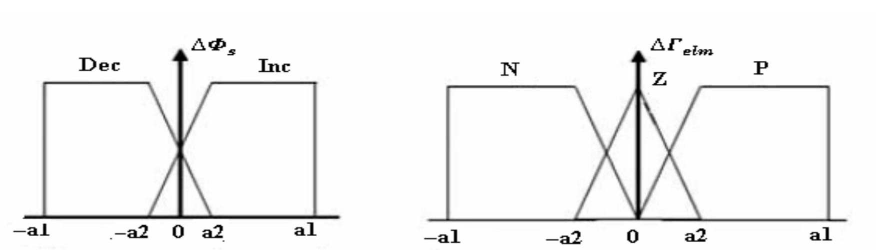

Fig. 17. Membership functions for ΔΦs and $\Delta\Gamma_{elm}$

We consider, in this case, two fuzzy sets functions (D: Decrease, I: Increase) for the stator flux and electromagnetic torque errors and three membership functions (N: Negative, Z: Zero, P: Positive) for the variation of the electromagnetic torque error.
The fuzzy rules of the argument fuzzy controller are presented in the following table.

Δθ		$\Delta\Phi_s$	
		Dec	Inc
$\Delta\Gamma_{elm}$	Dec	$\mu(-2\pi/3)$	$\mu(-\pi/3)$
	Inc	$\mu(2\pi/3)$	$\mu(\pi/3)$

Table 6. Fuzzy rules of argument controller

$\mu(\theta)$ is the membership function for the output variable of argument fuzzy controller defined as represented by the following figure.

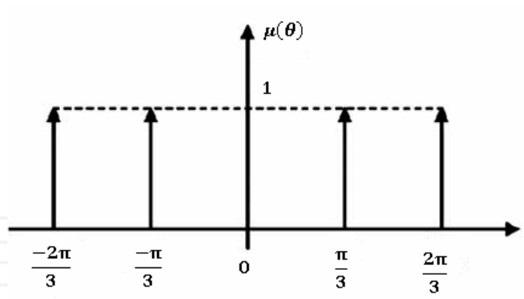

Fig. 18. Membership function for output argument controller

The voltage vectors in conventional DTC have constant amplitude in opposite with FDTC based space vector modulation where this amplitude is modified versus the torque and its derivative. Then, the fuzzy rules of the amplitude fuzzy controlled take form:
If $\Delta\Gamma_{elm}$ decrease and $d(\Delta\Gamma_{elm})/dt$ is negative then magnitude vector is small.
Consequently, these different rules are resumed in the following table, where the fuzzy sets used are, N: Negative, M: Medium, Z: Zero, P: Positive, S: Small and L: Large.

V		$\frac{d(\Delta\Gamma_{elm})}{dt}$		
		N	Z	P
$\Delta\Gamma_{elm}$	Dec	S	S	M
	Inc	M	L	L

Table 7. Fuzzy rules of amplitude fuzzy controller

Finally, the fuzzy sets of output magnitude fuzzy controller are defined by delta and trapezoidal membership functions as shown by this figure.

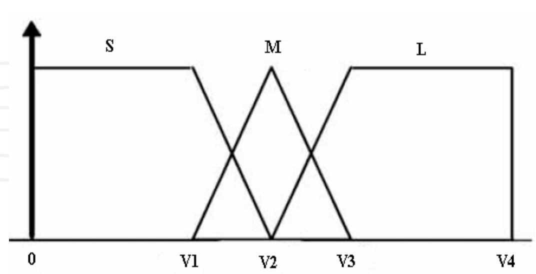

Fig. 19. Membership function for output magnitude controller

4.2 Direct torque control based artificial neural networks

Among the other intelligence techniques can improving the performance of system control and are recently showing good promise for applications in power electronics and motion control system, the use of Artificial Neural Network (ANN).

Different techniques based ANN are exploited for the control of IM; particularly, in the field of the IM Direct Torque Control, many types of these techniques are adopted. The most popular of ANN, used in DTC, is the multilayer feed forward network, trained by the back propagation algorithm, which is composed on the input layer, output layer, and several hidden layers.

Also, as the switching table has an important role in the DTC, for increasing the execution speed of the system, ANN is applied to emulate the classical switching table of the DTC obtaining the optimal switching patterns.

The switching table has as inputs the electromagnetic torque error, the stator flux error and the angle of the flux, and as output the voltage space vector to be generated by the inverter. Since this switching lookup table only depends on these inputs and not on the parameters of the IM, it can be trained off-line. Therefore, the inputs of switching table will be converted to digital signals, for reducing the training patterns and increasing the execution speed of the training process. Thus, one bit (1 or 0) represents the flux error, two bits (11 for state 1 , 00 for state 0 or 01 for state -1) the torque error and three bits the region of stator flux.

The structure of the ANN as a part of DTC is presented by figure 20, which has six inputs nodes corresponding to the digital variables (three for angle flux, one for flux error and two for torque error), six neurons in the first hidden layer, five neurons in the second hidden layer and three neurons in the output layer.

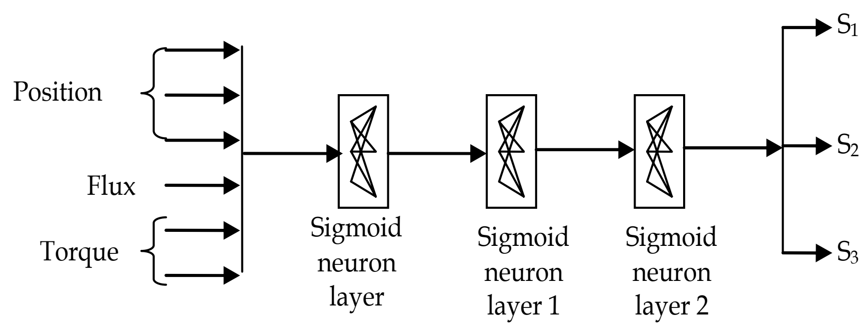

Fig. 20. Structure of the ANN

After completion of the training procedure, the network performance off-line with an arbitrary input pattern will be tested to ensure successful training. After that, the weights and biases are down-loaded to the prototype network substituting the traditional switching lookup table as a part of DTC.

An example of the ANN combined with Fuzzy inference system for the control of the IM speed will be presented in the next section.

5. Control of asynchronous motor speed based on a fuzzy / neural corrector

These last years, a most interest concerned the use of the artificial intelligence techniques (neural networks, fuzzy logic, genetic algorithms) which have the potential to provide an improved method of deriving non-linear models, have self adapting capabilities which make them well suitable to handle non-linearities, uncertainties and parameter variations.

The simplest of these methods are based on the learning of an already existing conventional controller; others methods operate a learning off-line of the process inverse model or of a reference model either completely on-line.

5.1 Description of the technique adopted for IM Speed control

As example, we have chosen to develop the case where a conventional neural controller (CNC) associated with a reference model (MRAS) for the learning phase is used to control the IM speed.
The parameters of the CNC are adjusted by minimising the error (e=u'-u) between the outputs of the MRAS and CNC as shown in the following figure.

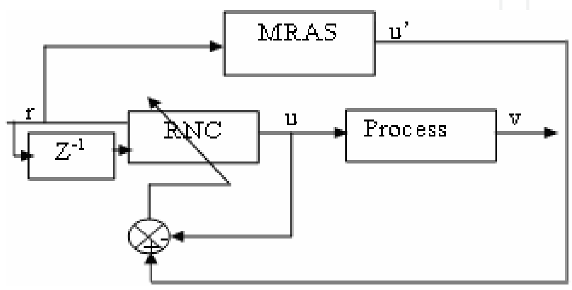

Fig. 21. Neural corrector for the IM speed control

Once the learning phase is carried out, the weights obtained are used for the neural controller, in the second phase, without the reference model.
Neural network, coupled with the fuzzy logic, speed control will be so efficient and robust. In this case, the reference model is represented by a fuzzy logic corrector (FLC) with two inputs: the error and the derivative of the error (next figure).

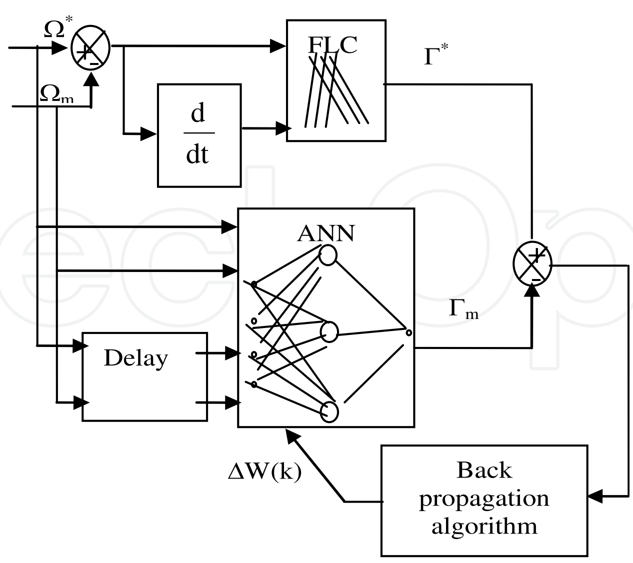

Fig. 22. IM Speed control based Fuzzy / neural corrector

The neural corrector architecture, shown by figure 23, presents 4 inputs, 3 neurons for the hidden coat with activation function type sigmoid and one output with linear activation function.

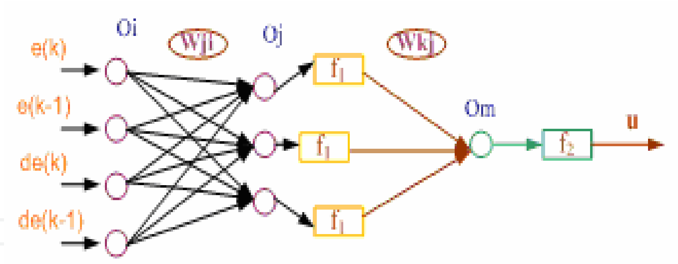

Fig. 23. Architecture of neural corrector

As it has been noted, a corrector type PI (Proportional Integral), for the reference model, which parameters are adapted by a fuzzy inference system, is used (Figure 24).

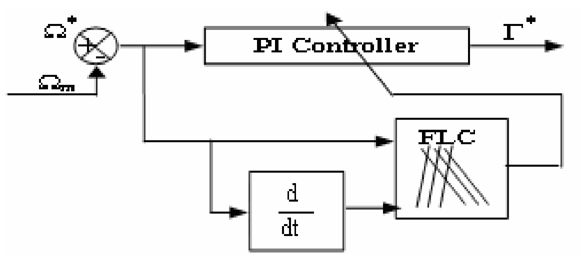

Fig. 24. Controller with PI structure adapted by fuzzy inference system

The PI parameters (Kp, Ki) are calculated by using the intermediate values (K'p and K'i) given by the fuzzy controller as follows:

$$\begin{aligned} K_p &= (K_{p_{\max}} - K_{p_{\min}})K_p^{'} + K_{p_{\min}} \\ K_i &= (K_{i_{\max}} - K_{i_{\min}})K_i^{'} + K_{i_{\min}} \end{aligned} \quad (8)$$

where the gains values are defined by using the Ziegler-Nichols method.
Both parameters (K'p, K'i), corresponding to the output of the system based on fuzzy logic, are meanwhile normalised in the range [0 1].

5.2 Simulation results

Simulations were performed to show the performances of the technique used in this section and based on fuzzy / neural corrector for the control of the DFIG speed. The ANN is a three-layer network in which the output layer has only one neuron corresponding to the reference torque value. The training procedure used was the Levenberg Marquardt back propagation algorithm. The weights are generated until the error between the calculated pattern and the desired pattern, corresponding to the output of the PI corrector used as reference model, which parameters are adapted by a fuzzy inference system, is very small and acceptable.
After this stage, the weights final values, corresponding to the steady state of the DFIG speed control, are saved and applied, in the second phase, steadily to the neural controller.
Approximations of ANN parameters are given here: Wij = 0.5 for i=1 to 3 and j=1 to 4
Wki for i=1,…3 are identical and constant in each interval depending on the DFIG speed (For this example, Wki = 0 in [0, 1.12], Wki = -7.4 in [1.12, 2],…)
These weights are applied to the neural controller without the reference model.

The following figure presents the model structure tested in Matlab / Simulink environment.

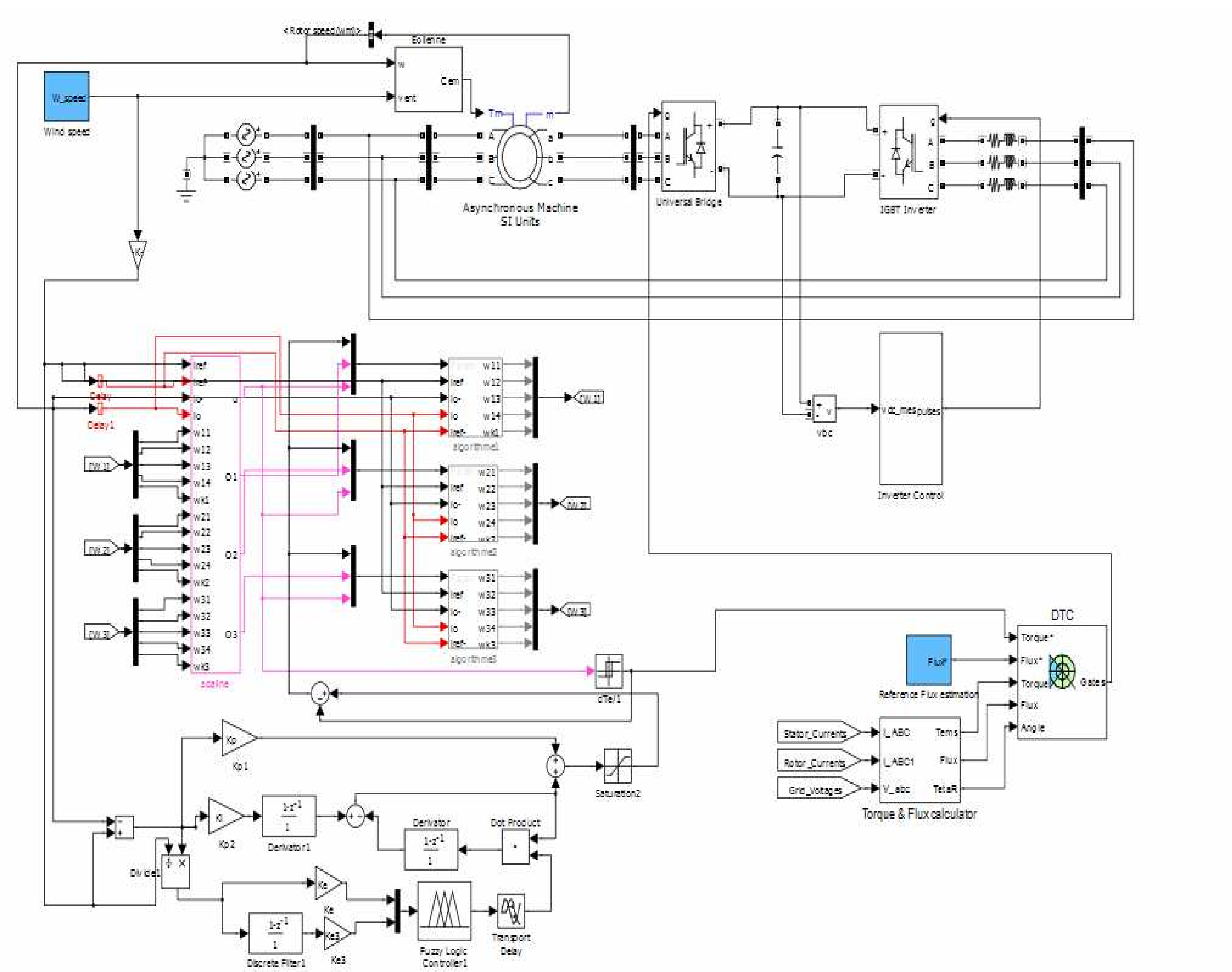

Fig. 25. Fuzzy neural corrector for the DFIG speed control (Simulink Model)

We have chosen to present the results corresponding to the rotation speed evolution and the electromagnetic torque.

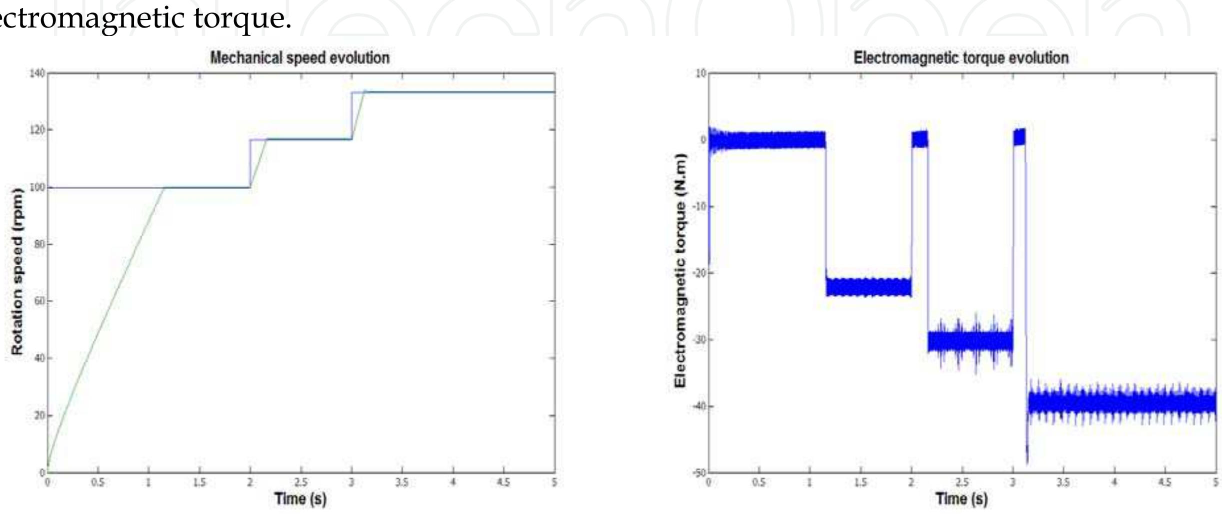

Fig. 26. Time evolution of speed and electromagnetic torque

We can note that mechanical speed track the reference values imposed and corresponding to different values of wind speed (Figure 26). Also the limitations in the torque are reduced.

6. Conclusion

The Direct Torque Control (DTC) is an important alternative method for the doubly fed induction generator drive, with its high performance and simplicity. Also, some techniques were developed in order to replace the conventional DTC switching table.
Another issue is concerned with the application of artificial intelligence techniques (fuzzy system, and neural network) to this machine control with DTC. Particularly, the application of these techniques for the selection of optimal voltage vectors will be developed.
Also, the control of the DFIG speed is realized by the technique of the artificial neural networks (ANN) with reference model. A controller based PI adapted by a fuzzy inference is used as reference model. Attention is focused on the dynamic performance of ANN speed control. The effectiveness of the proposed scheme control is demonstrated by simulation using the blocks PSB of Matlab / Simulink.
Finally, in this chapter, we can conclude that the DTC method applied to doubly fed induction generator for wind system and based artificial intelligence techniques present most interest and contribute to improvement of system response performances.
The first investigations, presented here, of the doubly fed induction machine control prove its effectiveness and its high dynamics. It will be completed in a future work by considering others control techniques.

7. References

Takahachi, I. & Noguchi, T. (1986). A new quick response and high efficiency control strategy of an induction motor. IEEE *Trans on Industry Application*, Vol.IA-22.N°5, pp 820-827, September/October 1986.

Baader, U. & Depenbroch, M. (1992). Direct Self Control (DSC) of inverter fed induction machine –A basis for speed control without speed measurement. IEEE. *Trans on Industry Application*. Vol.IA-288.N°3, pp 581-588, May/June 1992.

PUJOL, A.A. (2000). Improvement in direct torque control of induction motors. *Thesis of doctorate of the university polytechnic of Catalonia*, Spain, 2000.

Ozkop, E. & Okumus, H.I. (2008). Direct Torque Control of Induction Motor using Space Vector Modulation (SVM-DTC). MEPCON *12th International Middle-East, Power System Conference*, pp 368-372, March 2008.

Cirrinciane, M., Pucci, M. & Vitale, G. (2003). A Novel Direct Torque Control of Induction Motor Drive with a Three-Level Inverter. IEEE *Power Tech Conference Proceeding*, Vol.3, 7pp, Bologna, June 2003.

Xiying Ding, Qiang Liu, Xiaona Ma, Xiaona. He & Qing Hu (2007). The Fuzzy Direct Torque Control of Induction Motor based on Space Vector Modulation. *Third International Conference on, Natural Computation* ICNC 2007, Vol.4, pp 260-264, Aug.2007.

Guohan Lin & Zhiwei Xu (2009). Direct Torque Control of an Induction Motor using Neural Network. *1st International Conference on, Information Science and Engineering* (ICISE), pp 4827-4830, 28 December.2009.

Martins, A.C., Roboam, X., Meynard, T.A. & Carvaiho, A.C. (2002). Switching Frequency Imposition and Ripple Reduction in DTC Drives by using Multilevel Converter. IEEE *Trans, on Power Electronics*, Vol.17 N°2, March 2002.

Yang Xia & Oghanna, W. (1997). Study on Fuzzy control of induction machine with direct torque control approach. Industrial Electronics. ISIE 97, *Proceeding of the International Symposium*, Vol.2, pp 625-630, Jul.1997.

Yang, J., Ryan, M. & Power, J. (1994). Using Fuzzy Logic," Prentice Hall, 1994.

Kumar, R., Gupta, R.A., Bhangale, S.V. & Gothwal, H. (2008). Artificial Neural Network based Direct Torque Control of Induction Motor Drives. IETECH *Journal of Electrical Analysis*, Vol.2, N°3, pp 159-165, 2008.

Toufouti, R., Mezian, S. & Benalla, H. (2007). Direct Torque Control for Induction Motor using Intelligent Technique. *Journal of Theoretical and Applied Information Technology*, Vol.3, N°3, pp 35-44, 2007.

Dreyfus, G., Martinez, J., Samuelides, M., Gordon, M.B., Badran, F., Thiria, S. & Hérault, L. (2002). Réseaux de neurons : Méthodologie et applications. Editions Eyrolles, 2002.

Grabowski, P.Z., Kazmierkowski, M.P., Bose, B.K. & Blaabjerg, F. (2000). A simple Direct torque Neuro Fuzzy control of PWM Inverter fed Induction motor drive. IEEE *Trans. Electron*. 47 N° 4, pp 863-870, Aug 2000.

Viljamaa, P. (2000). Fuzzy gain scheduling and tuning of multivariable fuzzy control methods of fuzzy computing in control systems. *Thesis for the degree of doctor of technology, Temper University of technology*, Finland, 2000.

Barbara H. K. (2001). Stator and Rotor Flux Based Deadbeat Direct Torque Control of Induction Machines. IEEE *Industry Applications Society, Annual Meeting*, Chicago, September 30-October 4, 2001.

Casadei, D., Profumo, Serra, G. & Tani, A. (2002). FOC And DTC:Tox Viable Schemes For Induction Motors Torque Control. IEEE *trans.Power Electronics*. *On PE*, Vol.17, N°.5, Sept 2002.

Schibili, N., Nguyen, T. & Rufer, A. (1998). Three-Phase Multilevel Converter for High-Power Induction Motors. IEEE *trans. On Power Elect*. Vol. 13 N°.5, 1998.

Roboan, X. (1991). Variateur de vitesse pour machine asynchrone, Contrôle de la vitesse sans capteur mécanique. Thèse Doctorat de L'INPT, Toulouse, 1991.

Ould Abdeslam, D., Wira, P., Mercklé, J., Chapuis, Y.A. & Flieller, D. (2006). Stratégie neuromimétique d'identification et de commande d'un filtre actif parallèle. *Revue des Systèmes, Série Revue Internationale de Génie Electrique* (RS-RIGE), vol. 9, no. 1, pp 35-64, 2006.

Ould abdeslam, D. (2005). Techniques neuromimétiques pour la commande dans les systèmes électriques: application au filtrage actif parallèle. *Thèse de doctorat d'état en Electronique, Electrotechnique et Automatique*, Université de Batna, 2005.

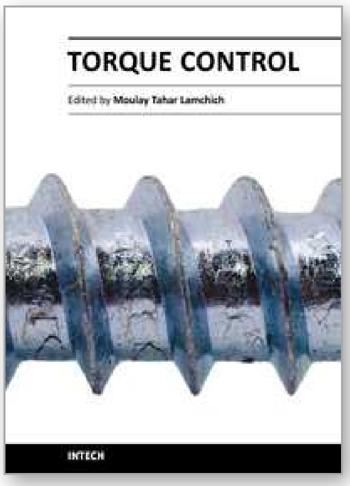

Torque Control

Edited by Prof. Moulay Tahar Lamchich

ISBN 978-953-307-428-3
Hard cover, 292 pages
Publisher InTech
Published online 10, February, 2011
Published in print edition February, 2011

This book is the result of inspirations and contributions from many researchers, a collection of 9 works, which are, in majority, focalised around the Direct Torque Control and may be comprised of three sections: different techniques for the control of asynchronous motors and double feed or double star induction machines, oriented approach of recent developments relating to the control of the Permanent Magnet Synchronous Motors, and special controller design and torque control of switched reluctance machine.

InTech Europe
University Campus STeP Ri
Slavka Krautzeka 83/A
51000 Rijeka, Croatia
Phone: +385 (51) 770 447
Fax: +385 (51) 686 166
www.intechopen.com

InTech China
Unit 405, Office Block, Hotel Equatorial Shanghai
No.65, Yan An Road (West), Shanghai, 200040, China
中国上海市延安西路65号上海国际贵都大饭店办公楼405单元
Phone: +86-21-62489820
Fax: +86-21-62489821